

Auto-focus for Compressively Sampled SAR

Shaun I. Kelly, Mehrdad Yaghoobi, and Mike E. Davies
 Institute for Digital Communications (IDCoM),
 University of Edinburgh, UK, EH9 3JL
 EMail: shaun.kelly@ed.ac.uk
 Telephone: +44 (0)131 6505659

Abstract—We investigate the effects of phase errors on a compressively sampled SAR aperture. We show that the standard methods of auto-focus, which are used as a post-processing step, are typically unsuitable for compressively sampled SAR. Instead of applying auto-focus as a post-processor we propose using a stable algorithm, which is based on algorithms from the dictionary learning literature, that corrects phase errors during the reconstruction and is found empirically to be effective at recovering sparse SAR images.

I. INTRODUCTION

Synthetic aperture radar (SAR) systems, due to limited computational resources and increasing resolution, generally do not process the received data on-board but instead store or transmit the data to the ground where the image formation process is performed. Systems are therefore constrained by on board storage capabilities and transmission links. An appealing idea is to apply the results of compressed sensing (CS) to reduce this constraint.

The theoretical results of CS are based on exact knowledge of the linear acquisition system, however, in practical situations, such a system cannot be known perfectly. This is the case in SAR where the received phase histories contain phase errors due to imperfect system modelling. Traditional SAR systems overcome these errors by post-processing the reconstructed image, a method which may not be compatible with CS.

The paper is organized as follows: in Section II we provide a model of the SAR acquisition system with phase errors. We then describe in Section III how classical methods can fit into the CS framework and their possible shortcomings. Inherent ambiguities in the CS/phase error problem are analysed in Section IV. A practical recovery algorithm for CS with phase errors is proposed in Section V. We then finish with some experimental results in Section VI to demonstrate the effectiveness of the proposed algorithm.

II. SAR PHASE ERROR MODEL

SAR systems which use dechirp-on-receive must estimate the round trip propagation delay to the scene centre at each position along the aperture. Errors in this estimate, which can be due to a non-idealised propagation medium or inaccuracies in the inertial navigation system, introduce unknown phase errors into the acquired data [1]. If not corrected, phase errors can degrade and produce distortions in the reconstructed image.

Adding a delay error τ_e into the SAR system model, produces a phase error $\phi_{\tau_e}(t) = (\alpha\tau_e^2 - \omega_0\tau_e) - 2\alpha\tau_e(t - \tau_0)$, where, t is the fast-time, τ_0 is the true propagation delay to the scene centre, 2α is the chirp rate and ω_0 is the carrier frequency. If we neglect the effects of the linear phase term, which is a valid approximation for narrow bandwidth systems, the discrete SAR observation model with phase errors becomes:

$$\mathbf{Y} = \text{diag}\{e^{j\phi}\}h(\mathbf{X}), \quad (1)$$

where, $h : \mathbb{C}^{M \times N} \rightarrow \mathbb{C}^{M' \times N'}$ is a linear map that models the SAR acquisition system, $\mathbf{Y} \in \mathbb{C}^{M' \times N'}$ are the phase histories,

$$\phi_m = \alpha\tau_{e_m}^2 - \omega_0\tau_{e_m} \quad (2)$$

are the phase errors and $\mathbf{X} \in \mathbb{C}^{M \times N}$ are the scene reflectivities.

If we further make a far-field and small aperture angle approximation the standard dechirped SAR acquisition system, e.g. see [1], can be modelled as a LHS and RHS matrix multiplication as in

$$\mathbf{Y} = \text{diag}\{e^{j\phi}\}\mathbf{A}\mathbf{X}\mathbf{B}, \quad (3)$$

where,

$$a_{mn} = \exp\left\{-j\left(\frac{2\pi(n-1)(m-1)}{M} - (n-1)\pi - (m-1)\pi + \frac{M\pi}{2}\right)\right\} \quad (4)$$

and

$$b_{mn} = \exp\left\{-j\left(\frac{2\pi(n-1)(m-1)}{N} - (n-1)\left(\frac{2\pi\omega_0}{2\alpha T} - \pi\right) - (m-1)\pi + \frac{N\pi}{2} - \frac{2\omega_0 L}{c}\right)\right\} \quad (5)$$

are the elements of the cross-range matrix $\mathbf{A} \in \mathbb{C}^{M \times M}$ and the range matrix $\mathbf{B} \in \mathbb{C}^{N \times N}$ respectively, where, L is the scene radius and T is the chirp period.

Clearly, without further assumptions, the problem of recovering ϕ and \mathbf{X} from \mathbf{Y} is ill-posed, since there are only MN equations and $N(M+1)$ unknowns.

III. CLASSICAL AUTO-FOCUS

Since, \mathbf{A} is essentially a Fourier matrix, we can rewrite the observation model in (3) as $\mathbf{Y} = \mathbf{A}\Phi\mathbf{X}\mathbf{B}$, where, Φ is a circulant matrix which can be viewed as a filter. Since \mathbf{A} and \mathbf{B} are invertible, we can recover $\Phi\mathbf{X}$ from \mathbf{Y} . Classical auto-focus methods such as the phase gradient auto-focus (PGA) algorithm [2] use the filtered image $\Phi\mathbf{X}$ to estimate \mathbf{X} by placing additional constraints on Φ and \mathbf{X} .

When \mathbf{Y} is compressively sampled in cross-range, the observation model is $\mathbf{Y} = \mathbf{A}'\Phi\mathbf{X}\mathbf{B}$, where $\mathbf{A}' \in \mathbb{C}^{S \times M}$ is a random $S < M$ row subset of \mathbf{A} . To recover $\Phi\mathbf{X}$ from \mathbf{Y} , CS theory provides us with a bound on the minimum number of samples required which is $S \geq CK_\Phi K_X \log^4(M)$ [3], where, C is a constant, K_Φ is the number of non-zero elements in the rows of Φ and K_X is the maximum number of non-zero elements in the columns of \mathbf{X} , therefore, it is clear that we require K_Φ times more compressive samples than if we had no phase errors. For this reason, in most cases, classical methods like the PGA algorithm are unsuitable for compressively sampled SAR.

IV. UNIQUENESS

Using ideas from the dictionary learning literature [4] we can define a set of sufficient conditions for the uniqueness of ϕ and \mathbf{X} given \mathbf{Y} . These conditions are:

- 1) the spark condition: any $2K_X$ columns of \mathbf{A}' are linearly independent
- 2) the columns of \mathbf{X} have exactly K_X non-zero elements,
- 3) for each of the $\binom{M}{K_X}$ possible K_X -sparse supports, there are at least $K_X + 1$ columns of \mathbf{X} ,
- 4) any $K_X + 1$ columns of \mathbf{X} , which share the same support, span a k -dimensional space,
- 5) any $K_X + 1$ columns of \mathbf{X} , which have different supports, span a $(K_X + 1)$ -dimensional space,

We define uniqueness up to a scalar α and a circular permutation \mathbf{P} of the true \mathbf{X} , i.e. $\tilde{\mathbf{X}} = \alpha\mathbf{P}\mathbf{X}$, which are the solutions to :

$$\begin{aligned} & \underset{\mathbf{X}, \mathbf{d}}{\text{minimise}} && \|\mathbf{X}\|_0 \\ & \text{subject to} && \text{diag}\{\mathbf{d}\}\mathbf{Y} = \mathbf{A}\mathbf{X}\mathbf{B} \\ & && d_m^* d_m = 1, m = 1, \dots, M, \end{aligned} \quad (6)$$

where, $\|\cdot\|_0$ measures the number of non-zeros matrix elements.

As is the case in dictionary learning, the richness condition 3 is completely unrealistic for compressively sampled SAR. However, this condition is only required for guaranteed uniqueness and from a probabilistic view point, is very pessimistic. It should also be noted that (6) requires combinatorial many operations to solve and is unsuitable for practical problems that involve noise.

V. ROBUST CONVEX RELAXATION

With the goal of designing an algorithm that is able to be solved in polynomial time and which is also robust to noise,

the non-convex function $\|\mathbf{X}\|_0$ in (6) can be replaced with its closest convex function $\|\mathbf{X}\|_1$ and the equality constraint can be replaced with an inequality constraint that accommodates noise, i.e.

$$\begin{aligned} & \underset{\mathbf{X}, \mathbf{d}}{\text{minimise}} && \|\mathbf{X}\|_1 \\ & \text{subject to} && \|\text{diag}\{\mathbf{d}\}\mathbf{Y} - \mathbf{A}\mathbf{X}\mathbf{B}\|_F \leq \sigma \\ & && d_m^* d_m = 1, m = 1, \dots, M, \end{aligned} \quad (7)$$

where, $\|\cdot\|_1$ is the sum of the absolute values of all matrix elements. Even though our objective function is now convex, (7) is still non-convex because the equality constraint is not linear and therefore does not define a convex feasible set.

A convenient formulation is to also move the inequality constraint to the objective to form the following Lagrangian:

$$\begin{aligned} & \underset{\mathbf{X}, \mathbf{d}}{\text{minimise}} && \|\text{diag}\{\mathbf{d}\}\mathbf{Y} - \mathbf{A}\mathbf{X}\mathbf{B}\|_F^2 + \lambda \|\mathbf{X}\|_1 \\ & \text{subject to} && d_m^* d_m = 1, m = 1, \dots, M, \end{aligned} \quad (8)$$

where, λ is a Lagrangian multiplier and there exists a one-to-one map, $\gamma : \sigma \rightarrow \lambda$ if $0 \leq \sigma \leq \|\mathbf{Y}\|_F$. The problem is still non-convex, however importantly, in each set of variables \mathbf{X} and \mathbf{d} –with the other fixed– we have a unique solution. This observation allows us to use a block relaxation type method which has been found to be effective in dictionary learning [5].

A. Majorisation Minimisation Method

Consider (8) when \mathbf{d} is fixed, i.e.

$$\underset{\mathbf{X}}{\text{minimise}} f(\mathbf{X}, \mathbf{d}) + \lambda \|\mathbf{X}\|_1, \quad (9)$$

where,

$$f(\mathbf{X}, \mathbf{d}) = \|\text{diag}\{\mathbf{d}\}\mathbf{Y} - \mathbf{A}\mathbf{X}\mathbf{B}\|_F^2. \quad (10)$$

A method used for solving (9) is a technique known as ‘‘majorisation minimisation’’. This technique replaces the objective function with a surrogate function that majorises the original objective and is much easier to solve. A function g is said to majorise f if $f(\omega) \leq g(\omega, \xi)$ and $f(\omega) = g(\omega, \omega), \forall \omega$ and $\xi \in \Upsilon$, where, Υ is the parameter space.

The surrogate function of $f(\mathbf{X}, \mathbf{d})$ can be developed using its Taylor series,

$$f(\mathbf{X}) = f(\mathbf{X}^\dagger) + df(\mathbf{X}^\dagger) + \frac{1}{2!} df^2(\mathbf{X}^\dagger), \quad (11)$$

where,

$$\overset{\rightarrow}{df}(\mathbf{X}) = \left\{ \frac{d}{dt} f(\mathbf{X} + t\mathbf{X}') \right\}_{t=0} \quad (12)$$

and

$$\overset{\rightarrow}{df^2}(\mathbf{X}) = \overset{\rightarrow}{df} \left(\overset{\rightarrow}{df}(\mathbf{X}) \right). \quad (13)$$

For our problem,

$$df^{\rightarrow \mathbf{X} - \mathbf{X}^\dagger}(\mathbf{X}^\dagger) = \text{tr} \left\{ 2 \text{Re} \left\{ \left(\mathbf{A} \left(\mathbf{X} - \mathbf{X}^\dagger \right) \mathbf{B} \right)^{\text{H}} \left(\mathbf{A} \mathbf{X}^\dagger \mathbf{B} - \text{diag} \{ \mathbf{d} \} \mathbf{Y} \right) \right\} \right\} \quad (14)$$

and

$$df^{\rightarrow \mathbf{X} - \mathbf{X}^\dagger}(\mathbf{X}^\dagger) = 2 \left\| \mathbf{A} \left(\mathbf{X} - \mathbf{X}^\dagger \right) \mathbf{B} \right\|_F^2. \quad (15)$$

Since f has bounded curvature, $df^{\rightarrow \mathbf{X} - \mathbf{X}^\dagger}(\mathbf{X}^\dagger) \leq L_f$ for $\left\| \mathbf{X} - \mathbf{X}^\dagger \right\|_F = 1$ and a finite constant L_f ,

$$\begin{aligned} f(\mathbf{X}, \mathbf{d}) &\leq \left\| \text{diag} \{ \mathbf{d} \} \mathbf{Y} - \mathbf{A} \mathbf{X}^\dagger \mathbf{B} \right\|_F^2 + \\ &\quad \text{tr} \left\{ 2 \text{Re} \left\{ \left(\mathbf{A} \left(\mathbf{X} - \mathbf{X}^\dagger \right) \mathbf{B} \right)^{\text{H}} \left(\mathbf{A} \mathbf{X}^\dagger \mathbf{B} - \text{diag} \{ \mathbf{d} \} \mathbf{Y} \right) \right\} \right\} + \\ &\quad \frac{L_f}{2} \left\| \mathbf{X} - \mathbf{X}^\dagger \right\|_F^2 \\ &\leq \left\| \text{diag} \{ \mathbf{d} \} \mathbf{Y} - \mathbf{A} \mathbf{X} \mathbf{B} \right\|_F^2 - \\ &\quad \left\| \mathbf{A} \left(\mathbf{X} - \mathbf{X}^\dagger \right) \mathbf{B} \right\|_F^2 + L \left\| \mathbf{X} - \mathbf{X}^\dagger \right\|_F^2, \end{aligned} \quad (16)$$

where, $L = L_f/2$. Therefore, we can define our surrogate function as

$$\begin{aligned} g(\mathbf{X}, \mathbf{X}^\dagger, \mathbf{d}) &= \left\| \text{diag} \{ \mathbf{d} \} \mathbf{Y} - \mathbf{A} \mathbf{X} \mathbf{B} \right\|_F^2 - \\ &\quad \left\| \mathbf{A} \left(\mathbf{X} - \mathbf{X}^\dagger \right) \mathbf{B} \right\|_F^2 + \\ &\quad L \left\| \mathbf{X} - \mathbf{X}^\dagger \right\|_F^2. \end{aligned} \quad (17)$$

Replacing the objective function with the surrogate function, (9) becomes

$$\underset{\mathbf{X}, \mathbf{X}^\dagger}{\text{minimise}} \quad g(\mathbf{X}, \mathbf{X}^\dagger, \mathbf{d}) + \lambda \left\| \mathbf{X} \right\|_1, \quad (18)$$

which is now a minimisation based on \mathbf{X} and \mathbf{X}^\dagger , where, if \mathbf{X} is fixed, the minimum of (18) occurs at $\mathbf{X}^\dagger = \mathbf{X}$ and if \mathbf{X}^\dagger is fixed the minimum occurs at

$$\{ \mathbf{X} \}_{i,j} = \mathcal{S}_\alpha(\mathbf{C}) = \begin{cases} c_{i,j} - \alpha \text{sign}(c_{i,j}) & \text{for } \alpha < |c_{i,j}| \\ 0 & \text{otherwise,} \end{cases} \quad (19)$$

where, $\mathbf{C} = \mathbf{X}^\dagger + \frac{1}{L} \mathbf{A}^{\text{H}} \left(\text{diag} \{ \mathbf{d} \} \mathbf{Y} - \mathbf{A} \mathbf{X}^\dagger \mathbf{B} \right) \mathbf{B}^{\text{H}}$ and $\alpha = \frac{\lambda}{2L}$.

By minimising (18) based on either \mathbf{X}^\dagger and \mathbf{X} in an alternating fashion, \mathbf{X}^\dagger and \mathbf{X} will converge to the solution of (9) at a sub-linear rate so long as $L \geq \left\| \mathbf{A} \right\|_2^2 \left\| \mathbf{B} \right\|_2^2$ [6]. In practice a feasible L can be determined using a back-tracking line-searching.

B. Phase Minimisation

Consider (8) when \mathbf{X} is fixed, which (ignoring constant terms) is given by:

$$\begin{aligned} &\underset{\mathbf{d}}{\text{minimise}} \quad \text{tr} \left\{ -2 \text{Re} \left\{ \text{diag} \{ \mathbf{d}^{\text{H}} \} \mathbf{A} \mathbf{X} \mathbf{B} \mathbf{Y}^{\text{H}} \right\} \right\} \\ &\text{subject to} \quad d_m^* d_m = 1, \quad m = 1, \dots, M. \end{aligned} \quad (20)$$

The unique solution of which is,

$$\mathbf{d} = e^{j \angle \text{diag} \{ \mathbf{A} \mathbf{X} \mathbf{B} \mathbf{Y}^{\text{H}} \}}. \quad (21)$$

C. Block relaxation Auto-focus

If we alternate between solving (9) and (20) in an alternating fashion this can be seen as a block relaxation of (8) the pseudo code of which is as follows:

Algorithm 1 $\mathcal{A}(\mathbf{X}, \mathbf{d})$

Output: \mathbf{X}, \mathbf{d}

repeat

$\mathbf{X}^\dagger \leftarrow \mathbf{X}$

$\mathbf{X} \leftarrow \mathcal{C}(\mathbf{X}, \mathbf{d})$

$\mathbf{d}^\dagger \leftarrow \mathbf{d}$

$\mathbf{d} \leftarrow e^{j \angle \text{diag} \{ \mathbf{A} \mathbf{X} \mathbf{B} \mathbf{Y}^{\text{H}} \}}$

until $\mathbf{X} - \mathbf{X}^\dagger < \text{threshold} \wedge \mathbf{d} - \mathbf{d}^\dagger < \text{threshold}$

Where, \mathcal{C} solves (9). The approaches used in [7] and [8] are of this form. This type of method is known to be stable assuming we have \mathcal{C} , i.e. we exactly solve (9) at each iteration. In practical systems where only an approximate solution at each iteration would be obtained, no stability analysis exists.

Another way to create a block relaxation is to consider the problem with three blocks of parameters, i.e.

$$\begin{aligned} &\underset{\mathbf{X}, \mathbf{X}^\dagger, \mathbf{d}}{\text{minimise}} \quad g(\mathbf{X}, \mathbf{X}^\dagger, \mathbf{d}) \\ &\text{subject to} \quad d_m^* d_m = 1, \quad m = 1, \dots, M. \end{aligned} \quad (22)$$

As long as (22) is minimised by varying \mathbf{X} followed by \mathbf{X}^\dagger the solution for each sub-problem is easily commutable and the complete algorithm is known to be stable and guaranteed to converge to an accumulation point or a connected set of accumulation points [5]. The pseudo code for this algorithm, when phase minimisation occurs at each iteration, is as follows:

Algorithm 2 $\mathcal{B}(\mathbf{X}, \mathbf{d})$

Initialise: $L \geq \left\| \mathbf{A} \right\|_2^2 \left\| \mathbf{B} \right\|_2^2$

Output: \mathbf{X}, \mathbf{d}

repeat

$\mathbf{X}^\dagger \leftarrow \mathbf{X}$

$\mathbf{C} \leftarrow \mathbf{X}^\dagger + \frac{1}{L} \mathbf{A}^{\text{H}} \left(\text{diag} \{ \mathbf{d} \} \mathbf{Y} - \mathbf{A} \mathbf{X}^\dagger \mathbf{B} \right) \mathbf{B}^{\text{H}}$

$\mathbf{X} \leftarrow \mathcal{S}_{\lambda/2L}(\mathbf{C})$

$\mathbf{d}^\dagger \leftarrow \mathbf{d}$

$\mathbf{d} \leftarrow e^{j \angle \text{diag} \{ \mathbf{A} \mathbf{X} \mathbf{B} \mathbf{Y}^{\text{H}} \}}$

until $\mathbf{X} - \mathbf{X}^\dagger < \text{threshold} \wedge \mathbf{d} - \mathbf{d}^\dagger < \text{threshold}$

It is interesting to note that this algorithm can be seen as a generalisation of Algorithm 1.

VI. EXPERIMENTAL RESULTS

In these experiments we investigate the performance of Algorithm 1 on compressively sampled phase histories that contain phase errors and compare its performance against a standard auto-focus method, PGA.

A. Synthetic Point-targets

In the first experiment we consider the model in (3) with a random 50% of the aperture positions. The scene consists of a small number of point targets with Gaussian clutter. Quadratic phase errors are added to simulate platform velocity measurement errors. The parameters for the synthetic model are in Table. I.

TABLE I
SAR SYSTEM PARAMETERS FOR SYNTHETIC EXPERIMENTS

parameter	value
carrier frequency (ω_0)	$2\pi \times 10 \times 10^9$ rad/s
chirp bandwidth ($2\alpha T$)	$2\pi \times 600 \times 10^6$ rad/s
scene radius (L)	50 m
number of targets	20
target to clutter ratio	50 dB
aperture sub-sampling ratio	0.5

Fig. 1(a) shows the reconstruction formed using the fast iterative shrinkage-thresholding algorithm (FISTA) followed by two iterations of the PGA algorithm (after which no improvement occurred). It has a target to background ratio (TBR) of 39.93 dB. Fig. 1(b) shows the reconstruction using Algorithm . It has a target to background ratio (TBR) of 72.13 dB. Fig. 1(c) shows the estimated phase errors for each method compared with the true phase errors. Algorithm estimates the phase errors more accurately than PGA, however, it still exhibits a constant phase estimate error due to the problem's inherent ambiguities which were described in Section IV.

B. GOTCHA Data Set

In this experiment we use a random 50% of the pulse data from 2 degrees the publicly available Gotcha data set [9] to simulate a compressively sampled aperture. To realistically model phase errors we added errors to the supplied aperture position data so errors in the distance to the scene centre were normally distributed with a variance of 1.7×10^{-6} meters. For this system the more general –non Fourier– model (3) is used, where we compute the forward model and its adjoint using the fast (re/back)-projection algorithms from [8]. Fig. 2(a) shows the reconstruction using FISTA. PGA was not used in this experiment because even with only two degrees of the Gotcha data set the phase errors are not approximately constant along the range axis, which is required in order to use PGA. Fig. 2(b) shows the reconstruction using Algorithm . The reduction in side lobes in Fig. 2(b) demonstrates clearly that Algorithm is doing an effective job of reconstructing the bright targets and correcting the phase errors in a realistic compressively sampled SAR problem.

VII. CONCLUSION

We have investigated the effects of phase errors on a compressively sampled SAR system. We have demonstrated that traditional SAR auto-focus methods that work as a post-processing measure are in most cases unsuitable. We have also proposed and demonstrated empirically, a stable algorithm that corrects phase errors and recovers a compressively sampled SAR image in a realistic scenario.

ACKNOWLEDGMENT

This work was supported in part by: EPSRC grants [EP/F039697/1, EP/H012370/1], the MOD University Defence Research Centre on Signal Processing and the European Commission through the SMALL project under FET-Open, grant number 225913.

REFERENCES

- [1] C. Jakowatz Jr, D. Wahl, P. Eichel, D. Ghiglia, and P. Thompson, *Spotlight-mode synthetic aperture radar: a signal processing approach*, 4th ed. Kluwer Academic Publishers, 1999.
- [2] D. Wahl, P. Eichel, D. Ghiglia, and C. Jakowatz Jr, "Phase gradient autofocus—a robust tool for high resolution SAR phase correction," *IEEE Trans. Aerosp. Electron. Syst.*, vol. 30, no. 3, pp. 827–835, Jul. 1994.
- [3] M. Rudelson and R. Vershynin, "On sparse reconstruction from Fourier and Gaussian measurements," *Comm. Pure Appl. Math.*, vol. 61, no. 8, pp. 1025–1045, Aug. 2008.
- [4] M. Aharon, M. Elad, and A. Bruckstein, "On the uniqueness of over-complete dictionaries, and a practical way to retrieve them," *J. Linear Algebra Appl.*, vol. 416, no. 1, pp. 48–67, Jul. 2006.
- [5] M. Yaghoobi, T. Blumensath, and M. Davies, "Dictionary learning for sparse approximations with the majorization method," *IEEE Trans. Signal Process.*, vol. 57, no. 6, pp. 2178–2191, Jun. 2009.
- [6] A. Beck and M. Teboulle, "A fast iterative shrinkage-thresholding algorithm for linear inverse problems," *SIAM J. on Imaging Sciences*, vol. 2, no. 1, pp. 183–202, Mar. 2009.
- [7] N. Onhon and M. Cetin, "A sparsity-driven approach for joint SAR imaging and phase error correction," *IEEE Trans. Image Process.*, vol. 21, no. 4, pp. 2075–2088, April 2012.
- [8] S. Kelly, G. Rilling, M. Davies, and B. Mulgrew, "Iterative image formation using fast (re/back)-projection for spotlight-mode SAR," in *Proc. of IEEE Radar Conf.*, May 2011, pp. 835–840.
- [9] C. Casteel Jr, L. Gorham, M. Minardi, S. Scarborough, K. Naidu, and U. Majumder, "A challenge problem for 2D/3D imaging of targets from a volumetric data set in an urban environment," in *Proc. SPIE, Algorithms for Synthetic Aperture Radar Imagery XIV*, April 2007.

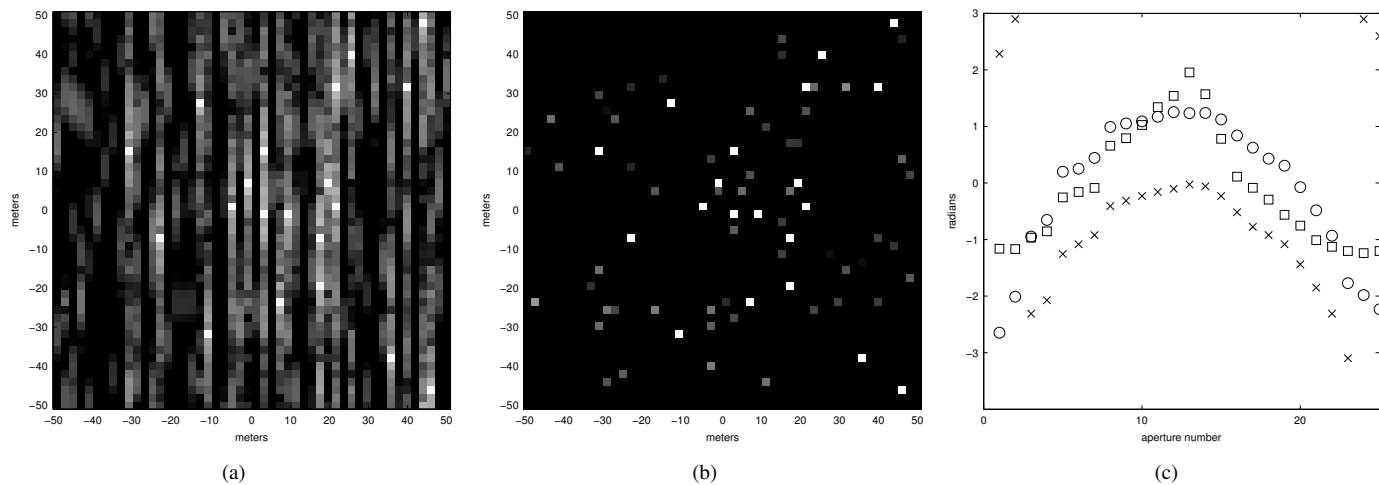


Fig. 1. point targets in clutter (a) reconstruction using FISTA followed by PGA (b) reconstruction using Algorithm (c) true phase errors 'x', PGA estimated phase errors '□' and Algorithm estimated phase errors 'o'

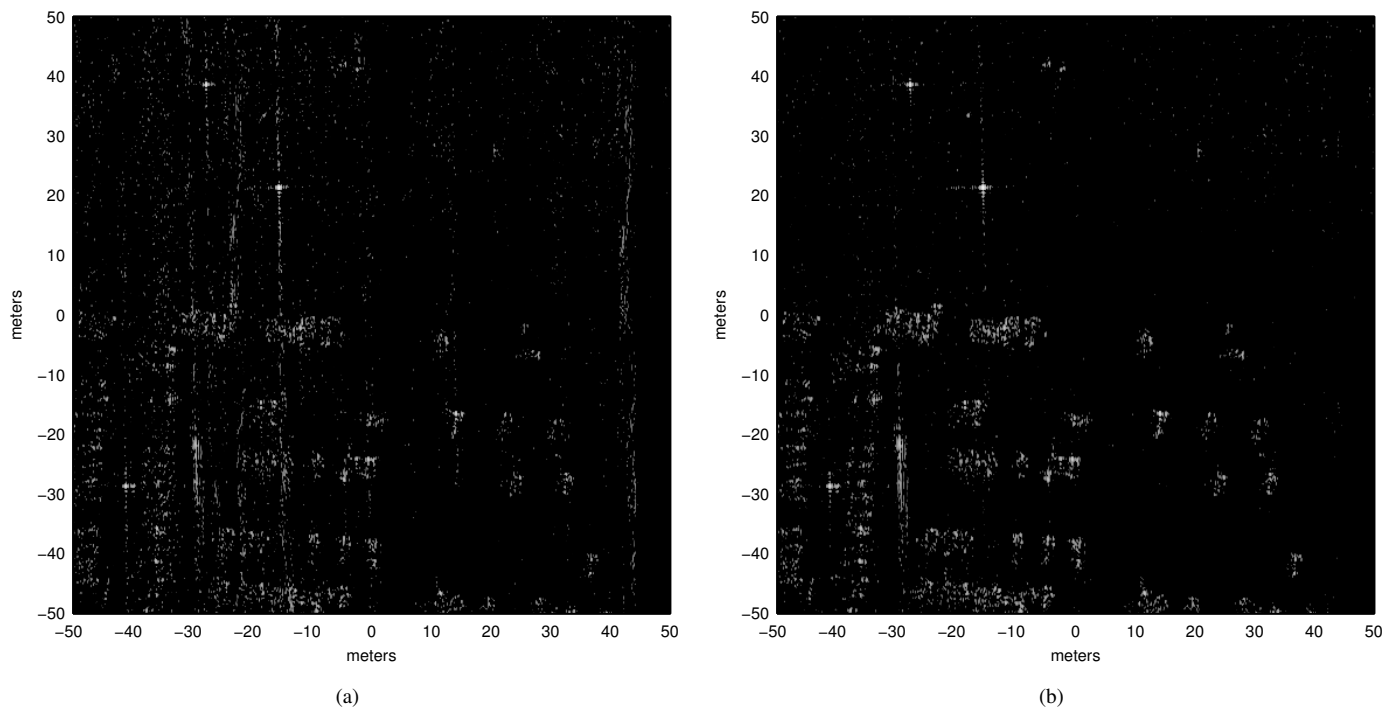


Fig. 2. reconstructions from 2° of the Gotcha data set with a compressively sampled aperture and phase errors. (a) reconstruction using FISTA (b) reconstruction using Algorithm focused